FUDMA Journal of Sciences (FJS)
ISSN online: 2616-1370
ISSN print: 2645 - 2944
Vol. 3 No. 2, June, 2019, pp 135 - 142

STRUCTURE OPTIMISATION OF THREE PHASES OF TITANIUM DIOXIDE

*Abdu, S. G., Shu'aibu, A. and Nura, H.

Department of Physics, Kaduna State University, Kaduna – Nigeria

Corresponding Author's Email: sgabdul@gmail.com

ABSTRACT

Titanium dioxide attracts great attention due to its many applications. It has been successfully employed in photocatalysis, paints, cosmetics, and medicine. It's used in the development of a high efficiency dye sensitized solar cell. In this work, the Fritz-Haber Institut *ab initio* Molecular Simulation code, FHI-aims was used to investigate and obtain the most stable ground state atomic coordinates of the three major phases of TiO_2.The exchange-correlation interactions are treated by the Linear Density Approximation. The ground state total energies were found to be; Rutile TiO_2 *-55653.8689758471 eV*, Anatase TiO_2 *-109308.048965066eV* and Brookite TiO_2 *-218614.36351209 eV*.

Keywords: Rutile TiO_2, Anatase TiO_2, Brookite TiO_2, Density Functional Theory, Geometry Optimization.

INTRODUCTION

Titanium dioxide is a naturally occurring oxide of titanium. It is a transition metal oxide and has various applications related to catalysis, electronics, photonics, cosmetics, etc. It is known to be a semiconducting metal oxide and forms three distinct crystal structure; Anatase, Brookite and Rutile. It is generally known that Rutile is thermodynamically the most stable phase, while Anatase and Brookite are metastable. The metastable phases of TiO_2 will go through phase transformation to Rutile at high temperatures (Hanaor and Sorrell, 2011). The Anatase and Rutile structures are well characterized by a distorted TiO_6 octahedral, and due to different bond lengths and angles between Titanium and Oxygen, they have different cell parameters and space groups. Anatase has $I4_1/amd$ space group with cell parameters of a=3.784Å and c=9.515Å, While Rutile has $P4_2/nm$ space group with cell parameters of a=4.5936Å and c=2.9587Å (Mo and Ching 1995, Cromer and Herrington 1995). Both structures are tetragonal. Brookite has an orthorhombic structure with *Pbca* space group and cell parameters of a=9.184Å, b=5.447Å, and c=5.145Å (Mo and Ching 1995, Samat *et al*., 2016).

TiO_2 is widely used in photo catalytic splitting of water into H_2 and O_2, which was discovered by Fujishima (1967), degradation of hazardous materials in the environment such as the reduction of CO_2 into hydrocarbon fuels (Indrakanti *et al*., 2009), and optical coating (Sankapal *et al*., 2005) due to its very high refractive index. It is relatively cheap, non-toxic and has a high chemical stability. It has applications in various industries like medicine, food additives and cosmetics as UV protection in sunscreens and many other products. TiO_2 has great promise in photovoltaic applications and is widely used for the fabrication of photoanodes in Dye Sensitized Solar Cells (DSSCs) (Barzykin and Tachiya 2002, Gratzel 2005, Haun *et al*., 1997).

Photocatalysis being one of the oldest discovered application of titanium dioxide has attracted immense attention since its discovery by Fujishima and Honda (1972). Since the discovery, photocatalysis has been a subject of serious research and exploration. Although Titanium dioxide (TiO_2) was the semi-conductor initially used, there are other semi-conducting material that have been identified and used but from all the available semi-conductors which can be used as photocatalysts, TiO_2 is generally considered to be the best photocatalyst available at present (Mills *et al*, 2002).

Titanium dioxide is mostly used in its two main phases, the most stable Rutile phase and Anatase phase, which under thermal treatment transforms to Rutile. Studies have shown that Rutile exhibits a narrower band-gap than Anatase, ~3.0 eV as compared with ~3.2 eV (Daude *et al*., 1977, Madhusudan *et al*., 2003). Studies show that the wide band-gap of TiO_2 limit its ability to interact well with the incoming visible light which is necessary for high performance under solar illumination. This leads to more research in the field to increase the visible light sensitivity through band gap modification (Bak *et al.*, 2002, Khan *et al.*, 2002) and increasing the active area exposed to light. A lot of interest has been pointed to the direction of nanostructures because of the large surface area exposable to sunlight, the high surface-to-volume ratio, non-toxicity, and the unique photochemical and photo-physical properties and also for their electron transport properties.

The ongoing research in Titanium dioxide is what motivated this work. The DFT based code, FHI-aims is used in performing the molecular relaxations/optimization which is significant for various theoretical and experimental investigations.

MATERIALS AND METHOD

Density Functional Theory

Density Functional Theory is a common technique used to study important properties of materials using computational method. It is a successful approach to finding solutions to the fundamental equation that describes the quantum behavior of atoms and molecules. It is based on the idea that all the ground state

properties of the system of interacting particles can be derived from the ground state electron density $n(\mathbf{r})$ of the system. In 1964 Hohenberg and Kohn formulated DFT as an exact theory of many-body systems: *For a system of interacting particles in an external potential, the external potential $V_{ext}(r)$is uniquely determined by the ground state density$n(r)$.* And *For any external potential $V_{ext}(r)$, we can define a universal functional or energy E[n] in the terms of density n(**r**), and the minimum for E[n] as a function of n(**r**), represents the exact ground state and the ground state density of the system.* (Martin 2014).

$$n(r) = N\int |\Psi(r, r_2, r_3 \ldots . r_N)|^2 dr, dr_2 \ldots . dr_N \quad (1)$$

The energy functional can now be formulated as

$$E_{HK} = T[n] + \int V_{ext}(r)\, n(r)\, d^3r + E_{11} \quad (2)$$

Where T[n] is the internal kinetic energy of the system, $V_{ext}(r)$ the external potential energy, and E_{11} represents the interaction energy of the nuclei.

In 1965 Kohn and Sham proposed an alternative approach and suggested that the complicated many-body problem can be replaced with an auxiliary independent-particle problem, which can be solved far more easily. This is based on the assumption that *the exact ground state of the system can be represented by the ground state of the auxiliary system of non-interacting particles and The auxiliary Hamiltonian can be selected so that it has a usual kinetic energy operator and an effective local potential V eff (**r**), which acts on the electron in the point **r**, having a spin of σ* (Martin 2014).

Using the Kohn-Sham approach, the Hohenberg-Kohn expression can be written as

$$E_{KS} = T_s[n] + \int V_{ext}(r)n(r)dr + E_{Hartree}[n] + E_{11} + E_{xc}[n] \quad (3)$$

$T_s[n]$ is the kinetic energy functional, $E_{Hartree}[n]$ is the classical Coulomb interaction energy of the electron density interacting with itself, E_{11} is the interaction between the nuclei, $V_{ext}(r)$is the external potential due to the nuclei and any other external fields, and $E_{xc}[n]$represents the exchange-correlation energy including all many-body effects.

The accuracy issues of DFT are strongly depended on the quality of the exchange correlation functional, because the exact exchange-correlation energy is not known generally, various approximations have been developed for the exchange correlation functional. These approximations include (i) Local Density Approximation, LDA, (ii) Generalized Gradient Approximation, GGA and (iii) Hybrid Approximation. The most common one used is the Local Density Approximation (LDA) (Kratzer *et al.,* 1999*,* Qing-Miao *et al.,* 2007*,* Juarez *et al.,* 2008). In LDA, the exchange correlation energy at each point in the system is the same as that of a uniform electron gas of the same density. Using this approximation, the exchange-correlation energy for a density$n(r)$is given by

$$E_{xc}^{LDA} = \int n(r)E_{xc}(n)d \quad (4)$$

FHI-aims

FHI-aims ("Fritz Haber Institute *ab initio* molecular simulations") is a computer program package for computational materials science based only on quantum-mechanical first principles (Blum *et al.*, 2009). The main production method is density functional theory to compute the total energy and derived quantities of molecular or solid condensed matter in its electronic ground state. In addition, FHI-aims can be used to describe electronic single quasi particle excitations in molecules using different self-energy formalisms (*GW* and MP2), and wave-function based molecular total energy calculation based on Hartree-Fock and many-body perturbation theory (MP2, RPA, SOSEX, or the more encompassing renormalized second-order perturbation theory, RPT2) (Blum *et al*., 2009).

FHI-aims requires two input files: the control.in which contains all runtime-specific information and the *Geometry.in* which contains only information directly related to the atomic structure for a given calculation. This includes atomic positions, with a description of the particulars of each element (or *species*) expected in control.in. In addition, lattice vectors may be defined if a periodic calculation is required. Any other information is only given here if it is directly tied to the atom in question, such as an initial charge, initial spin moment, relaxation constraint etc. The two input files must be placed in the same directory from where the FHI-aims binary file is invoked at the terminal. For more accuracy, FHI-aims provides pre-constructed default definitions for sub keywords associated with different species (chemical elements) which are useful in controlling the basis set, all integration grids, and the accuracy of the Hartree potential.

The initial structural parameters (lattice constants and the fractional coordinates) were obtained from material project (Jain *et al.,* 2011; Ong *et al.,* 2008), the parameters were optimized using 2 different xc-function. (LDA and PBE). A default control.in was made to relax the starting coordinates and lattice parameters of the 3 phases of Titanium dioxide using Bloyden-Fletcher Goldfarb-Shannon (BFGS) Algorithms. The relaxation was carried out in two stages with a convergence criterion tolerance of 10^{-2} eV/Å. The keyword 'relax_unit_cell' was added to the control.in to relax not just the atomic coordinates but also the unit cell shape.

RESULTS AND DISCUSSION

Structure Optimization

Tables 1 and 2 below give the optimized lattice constants for tetragonal Rutile TiO_2 and Anatase TiO_2 respectively. The

optimized lattices for orthorhombic Brookite TiO_2 is shown in Table 3.

Table 1: Optimized lattice constant of Rutile TiO_2

Method	Optimized Lattice Constant (Å) and Cell Volume (Å^3)		
	a(Å)	*c*(Å)	(Å^3)
LDA	4.543	2.927	60.42
PBE	4.644	2.972	64.12

Table 2: Optimized lattice constant of Anatase TiO_2

Method	Optimized Lattice Constant(Å) and Cell Volume (Å^3)		
	a(Å)	*c*(Å)	(Å^3)
LDA	3.730	9.500	132.18
PBE	3.799	9.745	140.70

Table 3: Optimized lattice constant of Brookite TiO_2

Method	Optimized Lattice Constants(Å) and Cell Volume (Å^3)			
	a(Å)	*b*(Å)	*c*(Å)	(Å^3)
LDA	5.078	5.395	9.115	249.79
PBE	5.172	5.513	9.273	264.19

Coordinates of the Starting Molecule

The initial coordinates generated are shown in Tables 4, 5 and Table 6, respectively. The Tables also show the final relaxed geometries using LDA.

Table 4: Atomic Coordinates of Rutile TiO_2

STRUCTURAL OPTIMISATION OF RUTILE TITANIUM DIOXIDE								
INTIAL GEOMETRY					FINAL GEOMETRY			
atom_frac	0.500000	0.500000	0.500000	Ti	atom_frac	0.504863	0.504896	0.507049
atom_frac	0.000000	0.000000	0.000000	Ti	atom_frac	0.007351	0.007385	0.011094
atom_frac	0.804580	0.195420	0.500000	O	atom_frac	0.800863	0.192984	0.508750
atom_frac	0.195420	0.804580	0.500000	O	atom_frac	0.193008	0.800874	0.508749
atom_frac	0.304580	0.304580	0.000000	O	atom_frac	0.301814	0.301806	0.009063
atom_frac	0.695420	0.695420	0.000000	O	atom_frac	0.693568	0.693527	0.008736

Table 5: Atomic Coordinates of Anatase TiO_2

STRUCTURAL OPTIMISATION OF ANATASE TITANIUM DIOXIDE								
INITIAL GEOMETRY					FINAL GEOMETRY			
atom_frac	0.000000	0.500000	0.250000	Ti	atom_frac	-0.000864	0.506066	0.249909
atom_frac	0.000000	0.000000	0.000000	Ti	atom_frac	-0.000534	0.006166	-0.000112
atom_frac	0.500000	0.000000	0.750000	Ti	atom_frac	0.499460	0.006163	0.749926
atom_frac	0.500000	0.500000	0.500000	Ti	atom_frac	0.499164	0.506058	0.499859
atom_frac	0.000000	0.500000	0.456163	O	atom_frac	-0.000852	0.506141	0.457872
atom_frac	0.500000	0.500000	0.293837	O	atom_frac	0.499139	0.506121	0.291948
atom_frac	0.000000	0.500000	0.043837	O	atom_frac	-0.000785	0.506096	0.041944
atom_frac	0.000000	0.000000	0.206163	O	atom_frac	-0.000775	0.006113	0.207892
atom_frac	0.500000	0.000000	0.956163	O	atom_frac	0.499283	0.006066	0.957884
atom_frac	0.000000	0.000000	0.793837	O	atom_frac	-0.000749	0.006103	0.791963
atom_frac	0.500000	0.000000	0.543837	O	atom_frac	0.499392	0.006119	0.541931
atom_frac	0.500000	0.500000	0.706163	O	atom_frac	0.499011	0.506103	0.707913

Table 6: Atomic Coordinates of Brookite TiO_2

STRUCTURAL OPTIMISATION OF BROOKITE TITANIUM DIOXIDE								
INITIAL GEOMETRY					FINAL GEOMETRY			
atom_frac	0.138146	0.407265	0.371013	Ti	atom_frac	0.139057	0.405057	0.371001
atom_frac	0.638146	0.592735	0.128987	Ti	atom_frac	0.638817	0.595017	0.129016
atom_frac	0.361854	0.907265	0.628987	Ti	atom_frac	0.361022	0.905153	0.629023
atom_frac	0.861854	0.092735	0.871013	Ti	atom_frac	0.861124	0.094967	0.870976
atom_frac	0.861854	0.592735	0.628987	Ti	atom_frac	0.860943	0.594943	0.629000
atom_frac	0.361854	0.407265	0.871013	Ti	atom_frac	0.361183	0.404983	0.870983
atom_frac	0.638146	0.092735	0.371013	Ti	atom_frac	0.638978	0.094847	0.370977
atom_frac	0.138146	0.907265	0.128987	Ti	atom_frac	0.138876	0.905033	0.129023
atom_frac	0.464315	0.391862	0.270273	O	atom_frac	0.465411	0.388711	0.269493
atom_frac	0.964315	0.608138	0.229727	O	atom_frac	0.965413	0.610825	0.230423
atom_frac	0.035685	0.891862	0.729727	O	atom_frac	0.034492	0.889264	0.730408
atom_frac	0.535685	0.108138	0.770273	O	atom_frac	0.534495	0.111209	0.769499
atom_frac	0.535685	0.608138	0.729727	O	atom_frac	0.534589	0.611290	0.730507
atom_frac	0.035685	0.391862	0.770273	O	atom_frac	0.034587	0.389175	0.769577
atom_frac	0.964315	0.108138	0.270273	O	atom_frac	0.965508	0.110735	0.269592
atom_frac	0.464315	0.891862	0.229727	O	atom_frac	0.465505	0.888792	0.230501
atom_frac	0.816566	0.851678	0.010307	O	atom_frac	0.815677	0.850980	0.010751
atom_frac	0.316566	0.148322	0.489693	O	atom_frac	0.315577	0.148929	0.489240
atom_frac	0.683434	0.351678	0.989693	O	atom_frac	0.684294	0.350997	0.989170

atom_frac	0.183434	0.648322	0.510307	O	atom_frac	0.184457	0.648963	0.510807
atom_frac	0.183434	0.148322	0.989693	O	atom_frac	0.184323	0.149020	0.989249
atom_frac	0.683434	0.851678	0.510307	O	atom_frac	0.684423	0.851071	0.510761
atom_frac	0.316566	0.648322	0.010307	O	atom_frac	0.315706	0.649003	0.010830
atom_frac	0.816566	0.351678	0.489693	O	atom_frac	0.815543	0.351037	0.489193

A summary of the relaxation process is given in Tables 7, 8 and 9 below:

Table 7: Summary of Relaxation of initial molecule (Rutile TiO_2)

Basis set	***Tier 1***	***Tier 2***
Total Energy (eV)	-54653.4820600366	-55653.868975371
No of self-consistence cycles	358	52
No of relaxation steps	29	4
Total Time (sec)	10368.229	26286.804

Table 8: Summary of Relaxation of initial Molecule (Anatase TiO_2)

Basis set	***Tier 1***	***Tier 2***
Total Energy (eV)	-109307.154835270	-109308.048965066
No of self-consistence cycles	467	383
No of relaxation steps	28	23
Total Time (sec)	21293.567	28820.53

Table 9: Summary of Relaxation of initial Molecule (Brookite TiO_2)

Basis set	***Tier 1***
Total Energy (eV)	-218614.36351209
No of self-consistence cycles	246
No of relaxation steps	19
Total Time (sec)	31283.441

The initial geometry of the three phases of Titanium dioxide were optimized employing the minimum basis (pre-relaxation using light species of element) and the optimized geometry was used as the starting geometry for the tier *2* basis (tight specie). The size of the basis set determines the accuracy of a calculation. The higher the size, the more accurate the result of the calculation, although it is computationally expensive. It can be seen from the results of relaxation in Tables 7 & 8 that a relaxation with tier 2 basis takes more time as compared with relaxation time of tier 1. It should be noted the relaxation of Brookite TiO_2 was done using tier 1 only. This is due to large number of atoms (24) as seen from the results it took about 8 hours for relaxation to be completed.

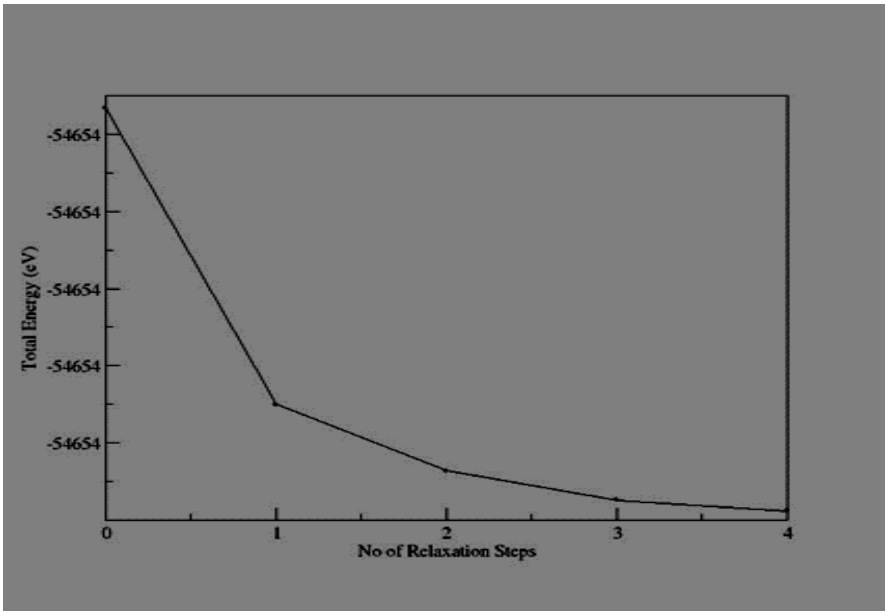

Fig. 1: Variation of energy with relaxation steps in Rutile TiO_2

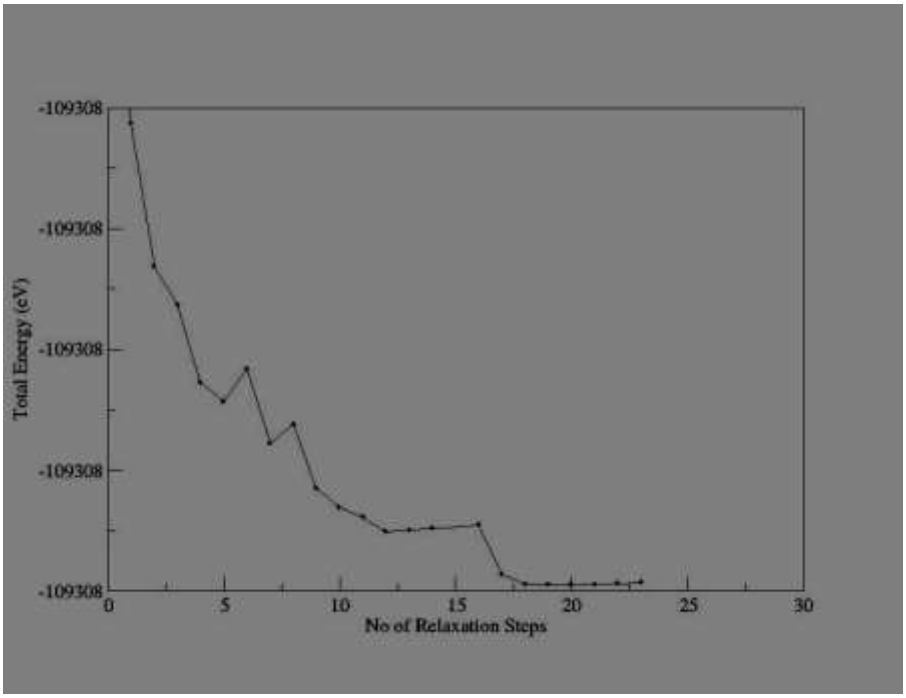

Fig. 2: Variation of Energy with Relaxation in Anatase TiO_2

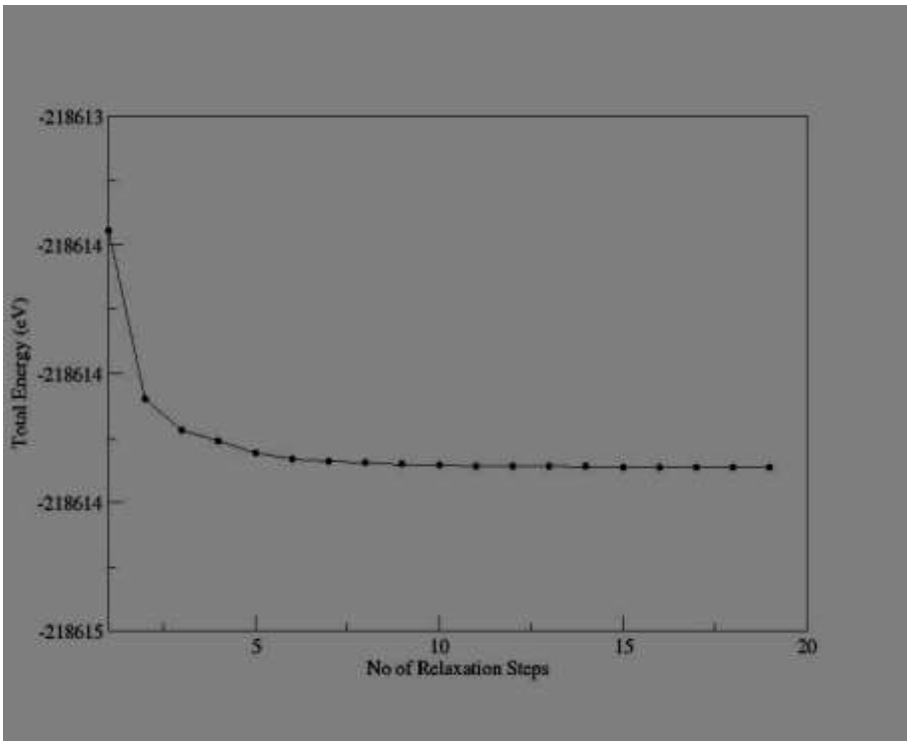

Fig. 3: Variation of Energy with Relaxation steps in Brookite TiO_2

CONCLUSION

As expected, the optimized lattice constants and structures provide better results as the total energy for two of the phases (Rutile TiO_2 and Anatase TiO_2) improved while increasing the basis. Figures 1, 2 and 3 show the changes in total energy as the molecules are relaxed. The result of the total energy calculation using the optimized geometries were found to be; -55653.8689758471 eV for Rutile TiO_2, -109308.048965066 eV for Anatase TiO_2 and -218614.36351209 eV for Brookite TiO_2.

REFERENCES

Bak, T. Nowotny, J. Rekas, M. Sorrell, C. (2002). Photochemical hydrogen generation from water using solar energy. *Int. J. Hydrogen Energy* 27(10); 991-1022.

Barzykin, A.V. and Tachiya, M. (2002). Mechanism of charge recombination in dye sensitized nanocrystalline semiconductors: Random flight model. *J Phys Chem B* 106: 4356-4363

Blum, V., Gehrke, R., Hanke, F., Havu, P., Havu, V., Ren, X., Reuter, K., & Scheffler, M. (2009). *Ab initio* molecular simulations with numeric atom-centered orbitals. *Computer Physics Communications, 180*, 2175-2196.

Cromer, D.T and Herrington, K. (1995). The structures of anatase and rutile," *J.Am. Chem. Soc.*, vol. 77, pp. 4708-4709.

Daude,N. Gout, C. and Jouanin, C.(1977). Electronic band structure of titanium dioxide. *Physical Review B* 15: 3229-3235

Gratzel, M. (2005). Solar energy conversion by dye-sensitized photovoltaic cells. *Inorg Chem* 44: 6841-6851

Hanaor, D.A. and Sorrell, C. (2011). Review of the Anatase to rutile phase transformation. *journal of material science* vol.114, no 19 pp.855-874

Hohenberg, P. and Kohn, W. (1964). Inhomogeneous Electron Gas *Physical Review* 136. B864.

Huang, S. Y. Schlichthorl, G. Nozik, A.J. Gratzel, M. and Frank, A.J (1997) Charge recombination in dye-sensitized nanocrystal-line TiO2 solar cells. *J Phys Chem* B 101: 2576-2582

Indrankanti, P.V, Kubiciki, D.J and Schobert, H.H. (2009). Photo induced activation of CO2 on Ti-based heterogeneous catalysts: current state, chemical physics-based insights and outlook *journal of energy and environmental science* vol 2, 745-758

Jain, A. Hautier, G. Ong, S. P. Moore, C. J. Fischer, C. C. Persson, K. A. and Ceder, G. (2011). Formation enthalpies by mixing GGA and GGA+ U calculations. *Physical Review B*, 84(4), 045115.

Juarez L. F. Da Silva1, and Catherine, S. (2008) Trends in adsorption of noble gases He, Ne, Ar, Kr, and Xe on Pd,,(111) : All-electron density-functional calculations, *physical review B* 77, 045401

Khan, S.M. Al-Shahry, M. Ingler, Jr. (2002). Efficient ph splitting by a chemical modified n-TiO_2 *Science* 297: 2243-2245.

Kohn, W. & Sham, L. J. (1965). Self-consistent equations including exchange and correlation effects. *Physical review,* 140(4A), A1133.

Kratzer, P. Morgan, C.G., Penev, E., Rosa, A.L., Schindlmayr, A., Wang, L.G., and Zywietz, T. (1999). FHI98MD Computer Code for Density Functional Theory Calculations for Poly-atomic Systems: User's Manual, Program Version 1:03

Madhusudan, Reddy, K. Manorama, S.V. and Ramachandra Reddy A (2003) Bandgap studies on anatase titanium dioxide nanoparticles. *Materials Chemistry & Physics* 78: 239-245

Martin, R.M (2014), *Electronic Structure: Basic Theory and Practical Methods*. Cambridge: Cambridge University Press, 1 ed.

Mo, S. and Ching, W.Y. (1995). Electronic and optical properties of three phases of titanium dioxide: Rutile, anatase, and brookite," *Phys. Rev. B*, vol. 51, pp. 13023-13032.

Ong, S. P. Wang, L. Kang, B. and Ceder, G. (2008). Li− Fe− P− O2 phase diagram from first principles calculations. *Chemistry of Materials,* 20(5):1798-1807.

Qing-Miao, H. Karsten, R. and Scheffler, M. (2007). Towards an Exact Treatment of Exchange and Correlation in Materials: "Application to the CO Adsorption Puzzle" and Other Systems. *Phys. Rev. Lett*. 98, 176103.

Samat,M.H, Adnan, N. Tarib, M.F, Hassan, O.H, Yahya, M.A and Ali, A.M. (2016). Structural, Electronic & Optical properties study of Brookite TiO2, *solid state science and technology.* Vol24: pp 107-120.

Sankapal, B.R, Lux-Steiner, M.C, Ennaoui, A. (2005). Synthesis and characterization of anatase-TiO_2 thin films. *Journal of applied surface science* 239 (2), 165-170